# A New Analytical Model for Heinrich Events and Climate Instability

CATHRINE SANDAL* AND DORON NOF+

*Department of Oceanography, The Florida State University, Tallahassee, Florida*

(Manuscript received 27 October 2006, in final form 25 May 2007)

ABSTRACT

The authors focus on Heinrich events and the question of whether the arrest and restart of convection can explain the associated sudden changes in oceanic and atmospheric temperature. For this purpose, a new (mixed) dynamical-box model is developed in which the ocean and atmosphere communicate via both Ekman layers and convection. The conservation of heat, salt, volume flux, and a "convection condition" yields a system of algebraic equations that are solved analytically. As expected, it is found that as the freshwater flux increases, the convective ocean temperature decreases. The heat flux from the ocean to the atmosphere, the transport of the oceanic meridional overturning cell (MOC), and the corresponding atmospheric flow generated by the heat flux from the ocean all decrease. However, the outgoing air temperature *increases* with increasing freshwater flux. This counterintuitive increase is because a decreased latent and sensible heat flux (to a humid atmosphere) means a reduced temperature difference between the warmer ocean and the cooler atmosphere, implying a cooler ocean and warmer atmosphere. For each wind speed, there is a critical freshwater flux beyond which the convection collapses and the temperatures of both the ocean and the air plunge because equatorial water is no longer flowing northward to replace the frigid northern waters. The above points to a potentially new instability process that was probably active during glaciation periods—when ice and snow are abundant, even the smallest amount of freshwater flux will cause local warming which, in turn, will cause increased melting, resulting in an ever-increased freshwater flux until the critical flux is reached and the MOC collapses. The model suggests that switching convection on and off changed the glacial ocean temperature by 4°C and the glacial air temperature by 12.5°C, both consistent with the Greenland Ice Sheet Project (GISP II) ice core record and the Centre Européen de Recherche et d'Enseignement des Géosciences de l'Environnement (CEREGE) alkenone record.

## 1. Introduction

It is often suggested that freshwater-induced reorganizations of the meridional overturning cell (MOC) are the cause of abrupt climate changes (Fig. 1). Both the Dansgaard–Oescheger (DO) and Heinrich events are frequently mentioned as processes associated with such changes (Bond et al. 1993; Broecker 1994; Blunier et al. 1998; Cacho et al. 1999; Bard et al. 2000; Boyle 2000; Labeyrie 2000; Marotzke 2000; Clark et al. 2002). Heinrich events (our focus here) are abrupt cold episodes occurring during the last glacial period. Other than the dramatic decrease in oceanic and atmospheric temperatures, their trademark is a relatively thick layer of ice-rafted debris (IRD) found in sediment cores in the North Atlantic. (This layer thins as one proceeds eastward in the North Atlantic.)

Ganapolski and Rahmstorf (2001, 2002), Rahmstorf (2002, 2003), and others suggested that instability of the MOC and the migration of the North Atlantic Deep Water (NADW) convection site southward during large (iceberg induced) freshwater fluxes into the North Atlantic are responsible for the DO and Heinrich events. Gildor and Tziperman (2003) argue, on the other hand, that such variations in the MOC are just too small to explain the temperature changes recorded by the proxies. Their idea is that (in part because of albedo) sea ice acts as an amplifier of the MOC fluctuations and that such an amplification is essential for explaining abrupt climate changes. Although several stud-

* Current affiliation: Bjerknes Center for Climate Research, Bergen, Norway.

+ Additional affiliation: Geophysical Fluid Dynamics Institute, The Florida State University, Tallahassee, Florida.

*Corresponding author address:* Doron Nof, 419 OSB, Dept. of Oceanography, The Florida State University, Tallahassee, FL 32306.

E-mail: nof@ocean.fsu.edu

DOI: 10.1175/2007JPO3722.1

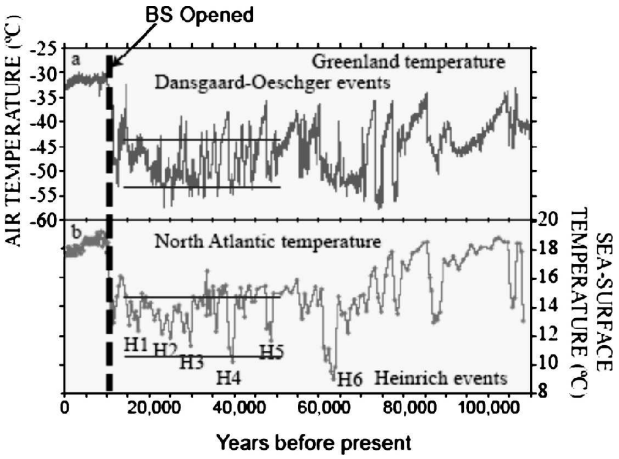


FIG. 1. Air and oceanic temperatures as determined from the Greenland GISP II ice core and the alkenone CEREGE record, respectively. The vertical distance between the straight horizontal lines indicates our theoretically calculated temperature changes for turning convection on and off. The lower line is simply adopted from the record for inactive convection, and the vertical distance between the two is calculated from the model. During the Heinrich events (marked with H), the Bering Strait (BS) was still closed (because of a lower sea level) so that the North Atlantic can be taken as a closed box. Note the different temperature scales for the ocean and atmosphere, and more importantly, note that on average the atmospheric fluctuations are 3–4 times larger than the oceanic. We shall argue that this is due to the water/air heat capacity ratio (4:1). [Record reproduced from De Boer and Nof (2004), who adapted part of it from Bard (2002).]

ies have supported this concept (see, e.g., Li et al. 2005; Timmerman et al. 2003; Wang and Mysak 2006; Loving and Vallis 2005; Kaspi et al. 2004; and the references therein), there is no consensus on the criticality of sea ice to abrupt climate change. Furthermore, even though some of the studies mentioned above employ what are usually referred to as "simple models," the models are not *that* simple, and for the typical reader, it is nearly impossible to personally verify how important sea ice really is. To make matters worse, some even question whether the heat flux released by the Gulf Stream (unrelated to the MOC) plays any role at all in warming the high latitudes (Seager et al. 2002).

Our present work will not bring a closure to the above debate but it will help clarify some important issues. The paper describes an analytical model involving merely heat exchange, convection, and Ekman layers. While it is not that easy to understand what the model implies (because of the nontrivial coupling to the atmosphere), since the model is analytical, it is very easy to tell which processes are important and which ones are not. Furthermore, it is a simple matter to tell whether the heat transported by the MOC is sufficient (by itself) to explain the temperature changes suggested by the proxies' analysis. Like all simple models, its major weakness is that it can only be used to obtain rough estimates of the processes at hand. Although there is no general agreement on how rough the estimates are, we feel that a careful choice of variables allows us to obtain results that are perhaps within 50% of the actual values. The main five issues that we wish to point out with our study are as follows:

(i) The ratio between the relatively large atmospheric temperature fluctuations and the relatively small oceanic fluctuations is roughly the same as the water/air heat capacity ratio (4:1). Hence, the heat capacity ratio acts as an amplifier of the small oceanic variations.
(ii) The amount of heat carried by an MOC of 10–20 Sv ($1\ \text{Sv} \equiv 10^6\ \text{m}^3\ \text{s}^{-1}$) is so large that it is sufficient to bring about the recorded variations in the temperature, provided that one compares an *active* state (where tropical water is brought to high latitude by the MOC) with an *inactive* state (where the MOC is not operational so that the frigid high-latitude water is not replaced by warmer water).
(iii) Heat-flux maps such as those presented by Hartmann (1994) suggest that radiation is not critical for turning convection on and off—only latent and sensible heat fluxes appear to be important for this process.
(iv) In view of (ii) and (iii) above, it appears that it is not essential to include sea ice in order to mimic the fluctuations calculated from the proxies.
(v) When the heat flux to the atmosphere is reduced because of an increased freshwater flux, the ocean cools and the atmosphere *warms*. However, the oceanic convection transmits the reduced amount of heat to a smaller amount of air so that, when horizontally mixed, the broader atmosphere cools.

Within our simply modeled steady North Atlantic box, mass, heat, and salt are conserved, a convection condition is invoked, and the box is coupled to the atmosphere through both the convection and the oceanic and atmospheric Ekman layers. The water entering the North Atlantic box originates in the South Atlantic and the Southern Ocean implying that our steady model represents averaging the dynamics over a *decadal* time scale. This means that important seasonal variations such as those associated with convection being on during the winter and off during the summer are not included here because our convective state corresponds to some (hypothetical) *mean* of summer and winter. Likewise, seasonal time-scale variations associated with the shift of the storm tracks and changing sea

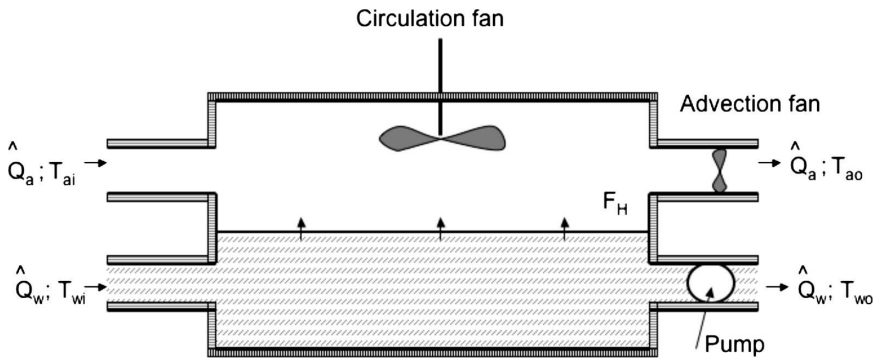


FIG. 2. The conceptual ultrasimple chamber model containing cold air flowing over warmer moving water. The advection fan controls the volume flux of the air whereas the pump controls the volume flux of the water. The circulation fan merely controls the speed of the air moving within the chamber so that it controls the vertical heat flux from the water to the air but not the horizontal volume transport. (Note that the direction of the atmospheric flow relative to the oceanic is unimportant—one flow can be opposing the other without affecting the outcome discussed in the text.)

ice cover (see, e.g., Denton et al. 2005) are not represented here.

Throughout this article we shall often speak about the convection in a time-dependent sense. This will not mean that we will be actually looking at a time-dependent problem, but rather that we will follow the changes that the fluid experiences as it gradually approaches the relatively small convective plumes [$\sim O(1$ km)] from a distance as far as a thousand kilometers away. We shall argue that it is the gradual heat loss that particles experience during this upstream journey that is critical for the convection.

We shall see that our model is consistent with Sandström (1908, 1916) thermodynamic theory. That theory states that no purely thermohaline circulation (i.e., cooling and heating only) can ever be established unless the heating source, which compensates for the cooling, takes place below the level of cooling—a situation that is virtually impossible to satisfy in the ocean because both the cooling and warming occur on the free surface (at approximately the same level). This restriction is circumvented here because our atmosphere does mechanical work on the ocean. This is achieved through the wind stress that is explicitly represented in the bulk heat-flux formulas and implicitly in the Ekman dynamics. Within the context of our model, this mechanical work need not be specified or solved for.

We also note that several MOC-recovery mechanisms have been proposed for the removal of a freshwater anomaly that temporarily terminates convection. Evaporative and dissipative processes could, within 100 yr, remove any freshwater anomalies restarting the convection (see, e.g., De Boer and Nof 2004). There are also negative feedbacks within the system. These include an increase in surface water density due to: increased sea ice and brine production (Paul and Schultz 2002); strengthening of local winds (from an enhanced equator to pole temperature gradient), which increase upwelling and surface salinity (Schiller et al. 1997); and increased heat loss from the ocean attributable to associated cooling of the atmosphere (Saravanan and McWilliams 1995). Although these removal mechanisms are important for the MOC recovery, they will not be addressed here.

### a. Chamber model

Before introducing the coupled model itself, it is useful to introduce the ultrasimple one-dimensional "chamber model" shown in Fig. 2. This ultrasimple model does not capture the role of freshwater fluxes nor does it include convection. It is merely introduced here to illustrate how the ocean and atmosphere exchange sensible and latent heat and to point out that some aspects of the associated heat-flux processes are counterintuitive. An insulated laboratory chamber contains a layer of air flowing over a moving layer of water. The air is removed from the chamber by an advection fan (pushing a volume flux $\hat{Q}_a$) and the water just below is forced out by a pump ($P$). The temperature of the incoming water (air) is $T_{wi}$ ($T_{ai}$) whereas the temperature of the outgoing water (air) is $T_{wo}$ ($T_{ao}$). As typical for most of the world ocean, the water is *warmer* than the air ($T_{wi} > T_{ai}$). While in contact with the atmosphere within the chamber, the ocean releases latent and sensible heat to the atmosphere so that the ocean cools ($T_{wi} > T_{wo}$) and the atmosphere warms ($T_{ai} < T_{ao}$).

Both the latent and sensible heat flux from the ocean

to the air are in part controlled by the circulation fan (attached to the chamber's ceiling), which merely affects the speed of the moving air within the chamber (but not the volume flux entering and leaving the chamber). Radiation is neglected in this chamber model, and as we shall see later, it will also be neglected later on because of the limited role that it plays in turning convection on and off. (This neglect will be justified later, not on the basis of scaling, but rather on the basis of relevance to convection.) For simplicity, we shall temporarily assume that the air is saturated but this assumption will be later relaxed.

Following Hartmann (1994), the sum of the total sensible and latent heat flux from the water to the air $F_H$ is

$$F_H = A\left[ C_S U(T_{\text{mean}} - T_{\text{air}}) + \frac{C_l}{B_e} U(T_{\text{mean}} - T_{\text{air}}) \right] C_{pa}\rho_a, \tag{1.1}$$

where $A$ is the area of the air–water interface, $\rho_w$ and $\rho_a$ (kg m$^{-3}$) are the densities of water and air, $C_{pw}$ and $C_{pa}$ (J kg$^{-1}$ K$^{-1}$) the specific heat capacities of water and air, $C_S$ and $C_L$ are constants associated with the sensible and latent heat fluxes, $U$ (m s$^{-1}$) is the wind speed above the surface, $B_e$ is the *equilibrium* Bowen ratio, $T_{\text{mean}}$ is the mean water temperature, and $T_{\text{air}}$ is the mean temperature of the air above, which gets in at $T_{ai}$ and leaves at $T_{ao}$. (For clarity, the conventional notation is defined in both the text and the appendix.) Also, $B_e$ depends on the mean water temperature in a nonlinear fashion but, as is frequently done, it will be taken, for the moment, to be constant.

We see from (1.1) that the heat exchange in question is proportional to the temperature difference between the water and the air, $(T_{\text{mean}} - T_{\text{air}})$. Hence, a reduced heat flux to the atmosphere means a reduced temperature difference between the warmer water and the cooler air, implying cooler water and warmer air. The above relationship (1.1) is an integrated relationship for the entire chamber. One can also write down the *local* heat flux $F_{HL}$ that involves the actual temperatures at each given cross section of the chamber,

$$F_{HL} = dA\left[ C_S U(T_w - T_a) + \frac{C_l}{B_e} U(T_w - T_a) \right] C_{pa}\rho_a, \tag{1.1a}$$

where $dA$ is an element surface area and the temperatures are now the local temperatures of the water and air.

Leaving the above relationships aside for a moment, we note that there is a second heat exchange relationship that equates the total heat loss from the water to the total heat gain of the atmosphere,

$$\rho_w \hat{Q}_w C_{pw}(T_{wi} - T_{wo}) = \rho_a \hat{Q}_a C_{pa}(T_{ao} - T_{ai}), \tag{1.2}$$

where $\hat{Q}_w$ and $\hat{Q}_a$ are the water and air volume fluxes. For simplicity, assume now that the pump and advection fan are set in such a way that the atmospheric and oceanic mass fluxes are the same (i.e., $\rho_w \hat{Q}_w = \rho_a \hat{Q}_a$). Under such conditions we get from (1.2)

$$T_{ao} - T_{ai} = \frac{C_{pw}}{C_{pa}} (T_{wi} - T_{wo}), \tag{1.3}$$

implying that the temperature gain of the atmosphere $(T_{ao} - T_{ai})$ is roughly four times larger than the oceanic temperature loss $(T_{wi} - T_{wo})$ because the air/water heat capacity ratio is approximately 1:4.

Using a few examples, we shall now show why the heat-flux properties can sometimes be counterintuitive. For the first example, say that the speed of the circulation fan is fixed, that the oceanic water enters at 20°C, the atmosphere enters with 2°C, and the ocean loses 3°C as the water moves through the chamber so that it exits at 17°C. Under such conditions, the atmosphere will warm 12°C (i.e., to 14°C), 4 times as much as the ocean has cooled. In this example, the temperature difference between the mean atmosphere (8°C) and the mean ocean (18.5°C) is 10.5°C. Note that the temperature difference between the ocean and the air has a maximum near the entrance and a minimum at the exit, so that the heat flux decreases gradually as one proceeds downstream. For a second example, we leave the entering water at the same temperature and increase the temperature of the incoming atmosphere to 8°C (instead of 2°C) so that the difference in the incoming fluids' temperatures is now smaller. This will decrease the heat flux from the ocean to the atmosphere so that the ocean will cool less than before and its exiting water will now be warmer than before (say, 18°C instead of 17°C). With less heat flux between the ocean and air, the atmosphere will gain less heat than before (8°C instead of 12°C), but the outgoing air temperature will now be warmer than before (at 16°C) simply because the atmosphere started with a higher temperature upstream. In this second example, the difference between the mean temperature of the ocean (19°C) and the mean temperature of the atmosphere (12°C) is 7°C, which is 3.5°C less than in the first example. This is consistent with our observation that a reduced heat-flux scenario implies warmer, not cooler, atmosphere. Further increases of the incoming air temperature further

decrease the heat flux and, hence, further increase the outgoing oceanic and atmospheric temperatures.

For the third example, consider again the incoming ocean and air temperatures of the first example, and suppose that the fan speed $U$ is now increased to the point when the ocean loses all of its heat to the atmosphere so that downstream, the ocean and atmosphere have the same temperature. (Taking the 4:1 ratio into account, we find that particular temperature to be 16.4°C.) Under such conditions, the heat flux near the entrance is larger than that of the first example because, although the temperature difference between the water and air is the same as that of the first example, the fan is now moving faster (i.e., $U$ is larger). This increased heat flux gradually decreases as one proceeds downstream and reaches zero at the exit where the temperature of the atmosphere and air are the same. All three examples do not directly relate to what happened when freshwater is added to the ocean, nor do they relate to convection, but they do illustrate the manner in which the ocean and atmosphere exchange heat.

The situation corresponding to equal mass fluxes in the ocean and atmosphere is not entirely hypothetical. We shall note later that this is the case for the atmospheric and oceanic Ekman layers, and it is probably for this reason that the atmospheric anomalies displayed in Fig. 1 are about 4 times greater than the corresponding oceanic anomalies. (The atmospheric and oceanic Ekman layers' mass flux is equal in magnitude but in opposite direction. However, this opposite-direction issue has no bearing on the issue at hand.) The Ekman layer connection to be employed later was originally proposed in isolation (i.e., in a form disjointed from other processes such as convection) by Nof et al. (2006), and an attempt will be made in section 2 to present it as clearly as possible without reproducing the details. It is important to realize upfront, however, that the Ekman coupling idea can be dropped altogether and replaced with the plausible assumption of equal mass transports in the atmosphere and ocean.

We shall see that our underlying precollapse MOC dynamics are as follows. Increased freshwater flux causes a reduction in the salinity that, in turn, implies a colder oceanic temperature (required for convection). The heat flux to the atmosphere decreases with increasing freshwater flux because of a significant reduction in the volume flux of the MOC (which overcompensates for the mild increase in the difference between the incoming and convecting water). Much of the discussion will be devoted to what variations in heat flux imply. As we just saw with the ultrasimple model, in the absence of radiation, the heat flux is proportional to the temperature difference between the ocean and the air, and since the ocean is usually warmer than the atmosphere (because the atmosphere is transparent to much of the sun radiation), a reduced heat flux is typically associated with a cooler ocean and a warmer atmosphere. However, under such conditions of a reduced heat flux to the atmosphere, the mass transport of the atmospheric flow involved in the heat exchange process is reduced significantly to compensate for the increased temperature.

### b. More on the relationship to earlier work

As mentioned, a wide range of numerical models has been used to investigate the cause and response of the MOC to freshwater fluxes in the North Atlantic (e.g., Rahmstorf et al. 2005; Stouffer et al. 2006; Manabe and Stouffer 1997; Schiller et al. 1997; Fanning and Weaver 1997). All of these models, as well as our present analytical effort, show that there exists a critical freshwater flux that causes a collapse of the MOC and a dramatic reduction in both the oceanic and the atmospheric temperatures. For increasing subcritical freshwater fluxes both our model and the numerics show a reduction in the heat flux to the atmosphere, but the complicated numerical models show that this decrease is associated with cooling whereas our model shows that it is associated with warming (of a much-reduced amount of air). This is not a contradiction—the local warming and reduced mass flux is merely "camouflaged" in the numerical atmosphere by mixing the air participating in the heat exchange process with neighboring air masses. Namely, we shall argue that, with a horizontal diffusivity as high as $10^6$ m$^2$ s$^{-1}$, a negative heat-flux anomaly over a 500 km $\times$ 500 km convection area will be mixed into a much larger region with lower mean temperatures within a few days.

Observed heat-flux variations around the globe suggest that, although radiation is obviously important to the global heat balance and, although it is of the same order as the latent and sensible heat flux, it is not important to turning convection on and off in the Atlantic. As the heat-flux maps displayed in Fig. 3 illustrate, the latent and sensible heat fluxes (Figs. 3b,c) for the Atlantic (where there is convection) and Pacific (where there is no convection) are dramatically different, indicating the critical role that both latent and sensible heat fluxes play in the convective heat exchange process. By sharp contrast, the net radiation heat fluxes in the two oceans (Fig. 3a) are almost identical, indicating that, despite the nonnegligible size of the radiation terms, radiation clearly does not play a critical role in the convection process. It will become clear later that the reason that radiation is not so important to the convection (turning on and off) is that the change in the atmo-

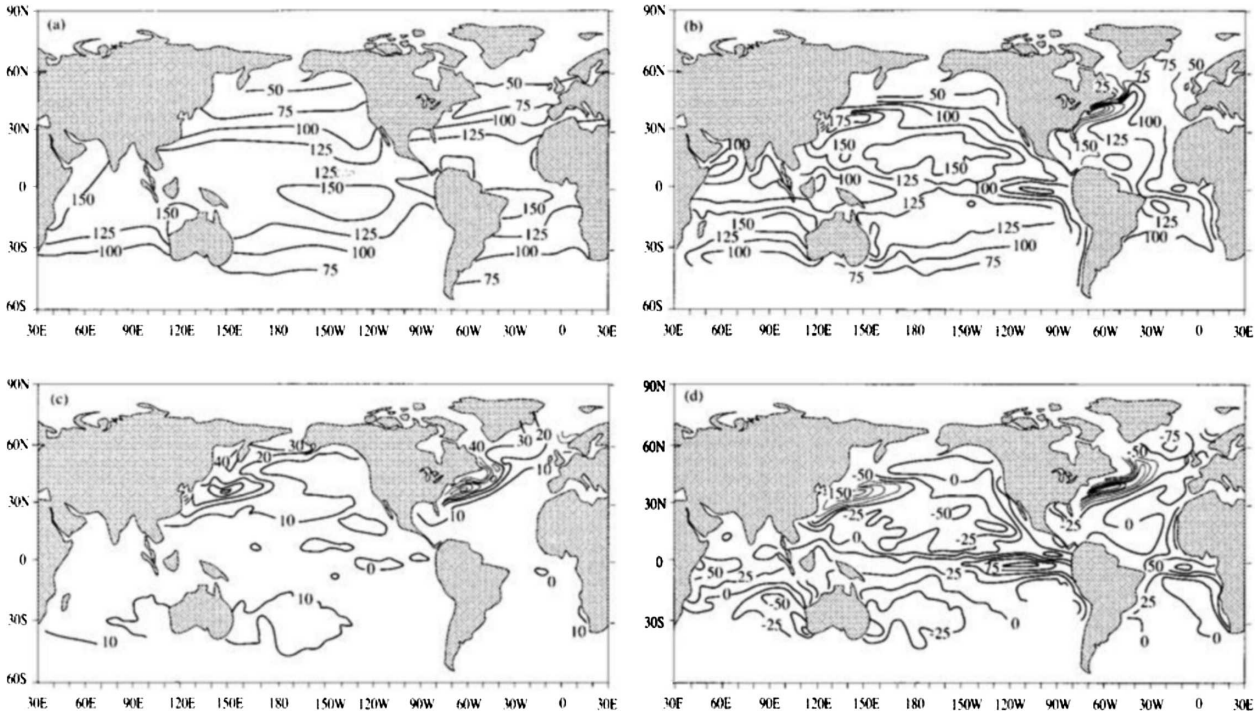


FIG. 3. Annual average heat-flux (W $m^{-2}$) maps for the World Ocean [reproduced from Hartmann (1994), who acknowledges adaptation from Oberhuber (1988)]: (a) net radiation, (b) latent heat flux, (c) sensible heat flux, and (d) net flux. Both the latent and the sensible heat fluxes show a dramatic difference between the North Atlantic (where there is convection) and the North Pacific (where there is no convection) indicating that both are important to NADW formation. By sharp contrast, the radiation map shows almost no difference, indicating that it is not very important to the convection. This is because, even though the radiation terms are not small, they depend primarily on the SST, which does not vary much (compared to the atmosphere) between convective and nonconvective states.

spheric temperature is much greater than that of the ocean (due to the much larger heat capacity of water), making the difference between the convective latent and sensible heat fluxes and nonconvective fluxes much more important than the variations in radiation.

On a related issue, it should also be pointed out in advance that the numerical models require a much larger freshwater flux to shut off convection than our analytical model. This is due to our particular choice of the controlling parameters that were close to a collapse state to begin with, and due to the wind-induced advection of water through the North Atlantic box, which numerical models include, but is not accounted for in our analytical model. Advection of water through the area of freshwater hosing will remove freshwater from the convection zone, requiring a larger flux to compensate for this loss.

Before proceeding and describing our model in detail, it is appropriate to mention here in passing that Nilsson and Walin (2001) showed that freshwater forcing in the North Atlantic could increase both circulation and convection in the region (because of changes in the equator-to-pole density gradient). A detailed comparison of their model to ours is impossible as Nilsson and Walin (2001) focus on entirely different processes. They use the advective–diffusive balance, with a scaling for the diapycnal flow between the two layers, whereas our model conserves mass, heat, and salt within the box incorporating a convection condition and a coupling to the atmosphere.

This paper is organized as follows. The coupled MOC model is presented in section 2, where we will view the North Atlantic as a box that receives warm and salty water from the South Atlantic (Fig. 4). The model equations are solved for an active (inactive) convection cell in section 3 (4) with a discussion and summary in section 5.

## 2. The coupled analytical model

The model (Fig. 4) is a combination of a dynamical aspect (used to derive the coupling between the ocean and atmosphere through the Ekman layers) and a conventional box model situated between 50° and 70°N. The general idea here is that the ocean and atmosphere communicate via Ekman layers that are active upstream of the [relatively small, $\sim O(1\text{ km})$] convection region and "prepare" the ocean surface for convection

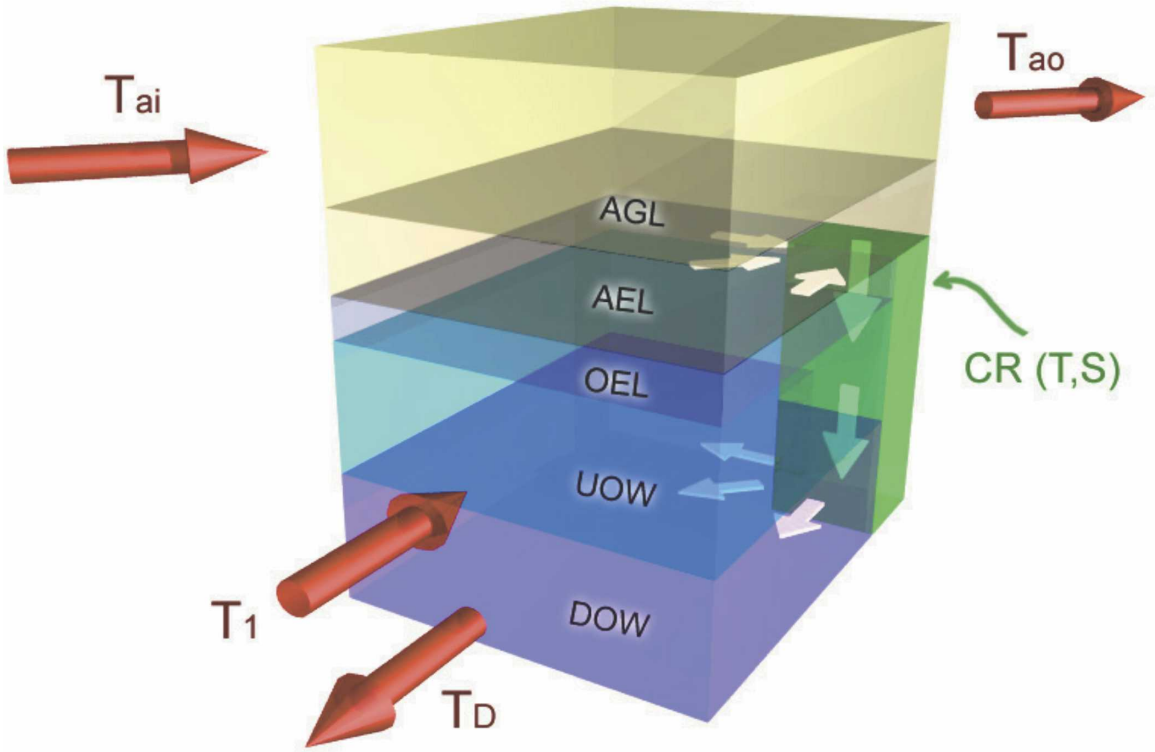


FIG. 4. A conceptual three-dimensional view of the coupled box model of the North Atlantic. AGL is the atmospheric geostrophic layer above the atmospheric Ekman layer (AEL). The flow in that layer is directed to the east whereas the surface atmospheric flow is toward the northeast, in accordance with Ekman-layer dynamics. OEL is the oceanic Ekman layer, UOW the upper ocean water, DOW the deep ocean water, CR the convection region (much smaller than the total area of the box and symbolically placed in the corner), $T_{ai}$ the temperature of the entering air (from the southwest), $T_{ao}$ the temperature of the exiting air, $T_1$ the temperature of the water entering the North Atlantic box from the south, and $T_D$ the temperature of the water below the North Atlantic box (the returning flow southward). The idea behind this conceptual model is that the ocean is brought into a convective state through the Ekman layers, which provide the "glue" between the atmosphere and the ocean allowing for the initial (nonconvective) transfer of heat upstream of the actual convection.

by cooling it down to the required convection temperature. Once convection sets in, other, much greater flows (i.e., flows that are superimposed on the oceanic Ekman layer) are generated (by the convection itself) and are drawn into the convection region. A similar process occurs in the atmosphere, where flows above the atmospheric Ekman layer are participating in the heat exchange, but we shall not be concerned with the question of how these flows are established. Namely, we implicitly assume that the atmosphere can accept all the heat released by the ocean. In accordance with all box models, the details of how or where the Ekman coupling actually takes place in relation to other dynamical processes within the box are not specified. We shall see that, in the limit of no Ekman coupling, the model reduces to the De Boer and Nof (2004) closed Bering Strait case, and, in the limit of no convection, the model reduces to the Ekman layers' connection of Nof et al. (2006). This indicates that the model is self-consistent.

### a. *Volume flux*

For steady flow, volume flux conservation within the box is given as

$$W = Q_1 + F_F, \tag{2.1}$$

where $W$ is the (unknown) volume flux of water that sinks from the upper to the deep layer, $Q_1$ is the (unknown) convection-induced transport of water from the Southern Ocean into the North Atlantic box, and $F_F$ is the (known) freshwater flux into the North Atlantic box (Fig. 4).

### b. *Salt conservation*

The conservation of salt is

$$(S_1 - S)Q_1 = SF_F, \tag{2.2}$$

where $S$ is the (unknown) salinity in the North Atlantic box and $S_1$ is the (known) salinity of the entering water from the south, $Q_1$.

*c. Heat*

NADW is formed in the box through cooling of all upper waters:

$$Q_1(T_1 - T) = \frac{A}{\rho_w C_{pw}}(F_S + F_L), \tag{2.3}$$

where

$$F_S = \rho_a C_{pa} C_S U_{10}(T_{\text{mean}} - T_{\text{air}}), \tag{2.4}$$

$$F_L = \rho_a L_e C_L U_{10} q^*(1 - R_H) + \rho_a C_L R_H \frac{C_{pa}}{B_e} \times U_{10}(T_{\text{mean}} - T_{\text{air}}), \tag{2.5}$$

$$T_{air} = \frac{T_{ai} + T_{ao}}{2}, \quad \text{and} \quad T_{\text{mean}} = \left(\frac{T_1 + T}{2}\right). \tag{2.6}$$

Here, $A$ ($m^2$) is the area of the North Atlantic box, $\rho_w$ and $\rho_a$ (kg $m^{-3}$) are the densities of water and air, $C_{pw}$ and $C_{pa}$ (J $kg^{-1}$ $K^{-1}$) are the specific heat capacities of water and air, $F_S$ and $F_L$ (W $m^{-2}$) are the sensible and latent heat fluxes, $C_S$ and $C_L$ are constants, $U_{10}$ (m $s^{-1}$) is the wind speed at 10 m above the surface, $q^*$ (g $kg^{-1}$) is the saturation specific humidity of the air, $L_e$ (J $kg^{-1}$) is the latent heat of evaporation, $R_H$ is relative humidity of the air, $B_e$ is the equilibrium Bowen ratio, $T_{\text{mean}}$ is the mean oceanic temperature of the box (as the water enters at $T_1$ and exits at $T$), $T$ is the (unknown) oceanic temperature in the North Atlantic box, and $T_{\text{air}}$ is the mean temperature of the air above the box, which gets in at $T_{ai}$ and leaves at $T_{ao}$, the (unknown) outgoing atmospheric temperature (Fig. 4). The above heat-flux parameterization follows the approach taken by Hartmann (1994). Also, $q^*$, $R_H$, and $B_e$ are all dependent on the mean air temperature $T_{\text{air}}$ in a nonlinear fashion. However, since we would like to use a linear equation in $T$, we have used the incoming air temperature $T_{ai}$ to calculate those three parameters. After completing our calculations we verified that this simplification introduces only minor and negligible changes in the six variables. Note that the heat flux associated with the freshwater flux has been neglected in (2.3), as the freshwater flux [$\sim O(0.1$ Sv)] is much smaller than $Q_1$ [$\sim O(10$ Sv)].

Several comments need to be made regarding (2.3). First, as alluded to earlier, the heat flux from the ocean to the atmosphere depends on the mean temperature difference between the ocean and the atmosphere. Also, the right-hand side of (2.3) shows that, in the limit of $U_{10}$ going to zero, there can be no convection because no heat can be removed from the ocean to the atmosphere. Second, the left-hand side of (2.3) shows that the heat flux is also the multiplication of the MOC's volume flux by the horizontal temperature difference. Third, (2.3) is the *total* heat equation involving both the Ekman layers (whose transport is much smaller than the MOC transport $Q_1$) and the water that is drawn in by the convection itself. Fourth, since the released heat is going to the atmosphere, one can also write an equation supplementary to (2.3) for the atmosphere:

$$\rho_a C_{pa} Q_{a1}(T_{ao} - T_{ai}) = \rho_w C_{pw} Q_1(T_1 - T), \tag{2.7}$$

where $Q_{a1}$ is the atmospheric flow participating in the heat exchange.

*d. Convection*

To allow water from the box to sink into the deep layer, we invoke the linearized convection condition,

$$T = T_D + \frac{\beta}{\alpha}(S - S_D), \tag{2.8}$$

where $\beta$ and $\alpha$ are the temperature and salinity expansion coefficients, respectively, and $T_D$ and $S_D$ are the temperature and salinity of the deep layer (below the thermocline), respectively (Fig. 4). [This convection condition was also used by De Boer and Nof (2004).]

*e. Ocean–atmosphere Ekman layer coupling*

The reader who is primarily interested in the results may wish to skip this subsection altogether and consider the ultrasimple chamber model described earlier in section 1a to be equivalent to the Ekman layers model discussed below. Another alternative is to a priori adopt the plausible assumption that the mass flux of the atmospheric flow involved in the heat exchange processes ($\rho_a Q_{a1}$) is equal to the oceanic mass flux generated by the convection ($\rho_w Q_1$) and substitute this condition into (2.7). The reader who, on the other hand, is interested in the Ekman layers details is referred to Nof et al. (2006), particularly to pages 424–425 and to their Fig. 3, where the basic coupling idea is discussed in isolation (i.e., without the incorporation of convection and freshwater fluxes).

The idea behind the coupling is that, upstream of the convection, the heat exchange between the ocean and the atmosphere occurs primarily through Ekman layers (insulated from their surroundings fluids) that prepare the surface water for convection. There is really no physical reason why other flows (such as the non-Ekman atmospheric geostrophic flow or upwelling and downwelling) cannot participate in the preparatory heat process but this is the simplest one-dimensional connection that one can think of and, it is for this reason that we adopt it.

Once convection starts, other water is drawn in and, ultimately, the MOC mass flux is much greater than the

original Ekman flux that prepared the ocean for convection in the first place. The oceanic Ekman flux $\tilde{Q}_w$ enters the box and cools as it goes through it from $T_{wi}$ to $T_{wo}$ (Fig. 4). The resultant heat is released to the atmosphere, warming the atmospheric Ekman layer from $T_{ai}$ to $T_{ao}$. We can write this heat exchange in terms of the one-dimensional conservation of heat in the direction perpendicular to the atmospheric geostrophic flow (see Fig. 3 in Nof et al. 2006),

$$\tilde{Q}_w \rho_w C_{pw}(T_{wi} - T_{wo}) = \tilde{Q}_a \rho_a C_{pa}(T_{ao} - T_{ai}), \quad (2.9)$$

where $\tilde{Q}_a$ and $\tilde{Q}_w$ are the atmospheric and oceanic volume Ekman fluxes entering the box.

Since the atmospheric and oceanic Ekman mass fluxes are in opposite direction but equal in magnitude (e.g., Gill 1982), we have

$$\rho_w \tilde{Q}_w = \rho_a \tilde{Q}_a. \quad (2.10)$$

Hence, relation (2.9) becomes identical to the coupling of the chamber model condition (1.3), where the downstream variables are replaced with the convection variables; that is, $T_1$ replaces $T_{wi}$ and $T$ replaces $T_{wo}$. Note that the opposite direction of the Ekman flows does not enter as long as we consistently use the upstream and downstream notation.

If we now assume that the Southern Ocean, deep Atlantic, and incoming air masses from the North American continent are infinitely large, their temperature and salinity are constants so that $T_1$, $T_2$, $T_D$, $T_{ai}$, $S_1$, $S_2$, and $S_D$ can all be taken as known. Also, $U_{10}$ is taken to be known because, just like the circulation fan of the chamber model, it affects the heat flux but not the transports. The five unknowns are $T_{ao}$, $T$, $S$, $W$, and $Q_1$, and as should be the case, we have five equations [(2.1), (2.2), (2.3), (2.8), and the coupling condition (1.3)] with the corresponding variables. We also assume here that the upwelling/downwelling due to the curl of the wind stress over the North Atlantic box region is much smaller than the convection at the site. Using typical observed monthly wind stress values, we calculated a mean upwelling in the North Atlantic box of 6 Sv, which is sufficiently small compared to the 20-Sv convection occurring in this region.

## 3. North Atlantic box, active convection

Substituting (2.8) into (2.2) gives a relation between $Q_1$ and $T$,

$$Q_1 = \frac{F_F\left[S_D + \frac{\alpha}{\beta}(T - T_D)\right]}{\left\{S_1 - \left[S_D + \frac{\alpha}{\beta}(T - T_D)\right]\right\}}, \quad (3.1)$$

that can be substituted into (2.3) to get

$$\frac{F_F\left[S_D + \frac{\alpha}{\beta}(T - T_D)\right]}{\left\{S_1 - \left[S_D + \frac{\alpha}{\beta}(T - T_D)\right]\right\}}(T_1 - T) = A_1[A_2(T_{\text{mean}} - T_{\text{air}}) + A_3], \quad (3.2)$$

where

$$A_1 = \frac{A\rho_a U_{10}}{\rho_w C_{pw}}, \quad A_2 = C_{pa}C_S + C_L R_H \frac{C_{pa}}{B_e}, \quad \text{and}$$

$$A_3 = L_e C_L q^*(1 - R_H).$$

Using (2.6) and the coupling condition to eliminate $T_{\text{air}}$ and $T_{\text{mean}}$ from (3.2) gives a quadratic equation for the unknown $T$:

$$A_6 T^2 + A_7 T + A_8 = 0, \quad (3.3)$$

where

$$A_6 = -\frac{\alpha}{\beta}[A_5 - F_F], \quad (3.4)$$

$$A_7 = A_1 A_2 \frac{\alpha}{\beta}\left[T_{ai} + \left(\frac{C_{pw}}{C_{pa}} - 1\right)\frac{T_1}{2}\right] + F_F\left[S_D - \frac{\alpha}{\beta}(T_1 + T_D)\right] + A_4 A_5 - A_1 A_3 \frac{\alpha}{\beta}, \quad \text{and} \quad (3.5)$$

$$A_8 = A_1 A_4\left\{A_3 - A_2\left[T_{ai} + \left(\frac{C_{pw}}{C_{pa}} - 1\right)\frac{T_1}{2}\right]\right\} - F_F T_1\left(S_D - \frac{\alpha}{\beta}T_D\right) \quad (3.6)$$

with

$$A_4 = \left(S_1 - S_D + \frac{\alpha}{\beta}T_D\right), \quad \text{and}$$

$$A_5 = \frac{A_1 A_2}{2}\left(1 + \frac{C_{pw}}{C_{pa}}\right).$$

Our desired solution to (3.3) must, of course, satisfy the limit $S \to S_1$ as $F_F \to 0$. This limit eliminates one of the roots, leaving us with only one physically relevant solution. Our chosen last glacial maximum (LGM) parameters are $A = 10^{12}$ m$^2$ (corresponding to 1000 × 1000 km$^2$), $\rho_w = 1000$ kg m$^{-3}$, $\rho_a = 1.5$ kg m$^{-3}$, $C_{pw} = 4000$ J kg$^{-1}$ K$^{-1}$, $C_{pa} = 1030$ J kg$^{-1}$ K$^{-1}$, $\alpha = 5 \times 10^{-5}$ K$^{-1}$, $\beta = 8 \times 10^{-4}$ K psu$^{-1}$, $L_e = 2.5 \times 10^6$ J kg$^{-1}$, $C_s = 9 \times 10^{-4}$, $C_L = 1.35 \times 10^{-3}$, $U_{10} = 5.0$ m s$^{-1}$, $R_H = 0.76$, $B_e = 0.6$, $q^* = 10$ g kg$^{-1}$, $T_{ai} = 5$°C, $T_1 = 18$°C, $T_D = 1.5$°C, $S_1 = 36.15$ psu, $S_D = 35.4$ psu, and

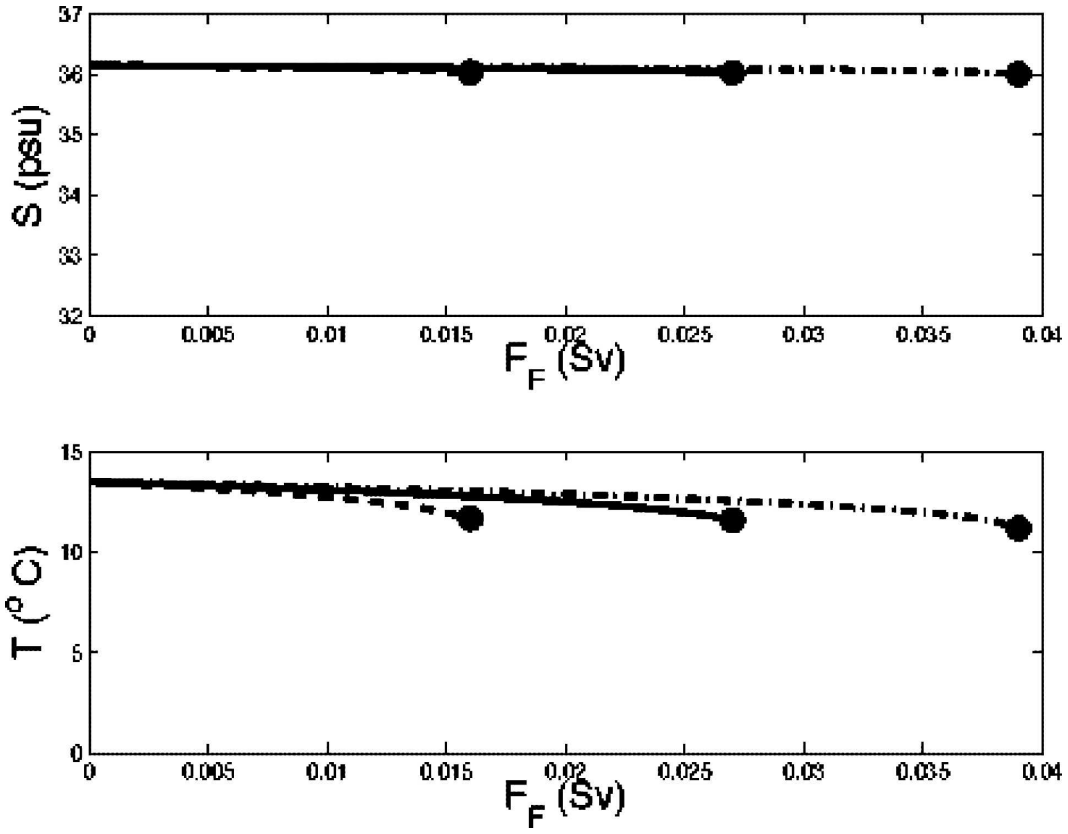


FIG. 5. The salinity and temperature as a function of the freshwater flux, $F_F$, for three different values of $U_{10}$: 3 m s$^{-1}$ (dashed line), 5 m s$^{-1}$ (solid line), and 7 m s$^{-1}$ (dashed–dotted line). The termination of the curves corresponds to the critical freshwater flux where the solution breaks down (solid dots). Note that a hypothetical iceberg 10 km $\times$ 10 km $\times$ 1 km melting during a period of two months produces about 0.02 Sv, which is sufficient to collapse the system. Also, note that since the water entering the box is 18°C and the convecting water is at most 13°C, the ocean cools at least 5°C due to the convection.

$0 \leq F_F \leq 4 \times 10^4$ m$^3$ s$^{-1}$ (see, e.g., Yin and Battisti 2001; Adkins et al. 2002; Schmidt et al. 2004).

At the limit of $F_F \to 0$, we have the initial condition $T_{F_F} = 0 = 13.5$°C. For $F_F = 0$ the two roots of the quadratic are 13.5° and 9.6°C. The second root is rejected as it does not satisfy the limit mentioned above. Since there is only one physically relevant solution for each freshwater flux, there are no multiequilibria for convection in the North Atlantic. This is because the Southern Ocean source for the North Atlantic box is taken here to be infinitely large so that Stommel's (1961) feedback mechanism has essentially been filtered out a priori. An important aspect of our solution is that there is a critical value for $F_F$ beyond which there is no solution (i.e., both roots become complex) because, for each $U_{10}$, there is a limit on the heat flux that can be transferred to the atmosphere. Note that this criticality is not related to the familiar criticality associated with the impossibility of cooling water below the freezing point, nor is it related to the criticality associated with strong winds pushing the water away from the convection zone (De Boer and Nof 2004).

Using the physically relevant root, the remaining four variables were calculated as a function of $F_F$ and plotted in Figs. 5–8 Since the solutions depend on $U_{10}$, upper ($U_{10} = 7$ m s$^{-1}$) and lower ($U_{10} = 3$ m s$^{-1}$) limits are also shown (dashed and dashed–dotted lines). We see that, for an increasing subcritical freshwater flux, the salinity decreases, decreasing ocean temperature to fulfill the convection requirement. Furthermore, the total amount of water that convects decreases, decreasing $F_H$ (Fig. 6; heat flux out of the North Atlantic box) as well as $Q_1$ (Fig. 7), the transport of water from the south into the North Atlantic box. This decrease in total heat flux is because $F_H$ is a combination of both $Q_1$ and $\Delta T$. Its decrease merely reflects $Q_1$'s dominance over the temperature difference in the heat-flux term. In other words, $Q_1$ decreases more rapidly than the temperature difference increases (when $F_F$ increases). Outgoing air temperature increases because, as in the

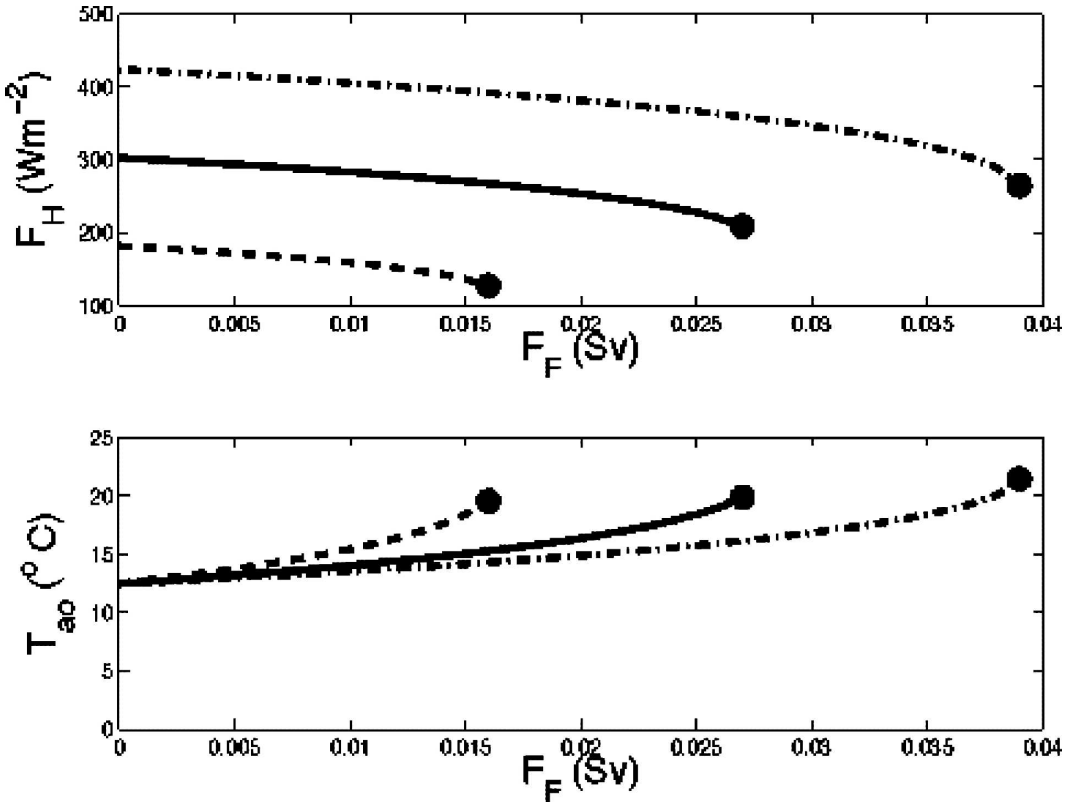


FIG. 6. As in Fig. 5, but for the heat flux $F_H$ and the outgoing air temperature $T_{ao}$. Note that since the air entering the box from the west has a temperature of $-5°$ and the outgoing air is at least 12.5°C (for $F_F = 0$), the air warms at least 17.5°C due to the convection. As before, solid dots indicate that the solution breaks down.

chamber model, a reduction in heat flux means that the warm ocean (relative to the atmosphere) will cool and the cool atmosphere will warm so that the temperature difference between the mean oceanic and atmospheric temperatures will be smaller than before. This is consistent with the Ekman exchange scenario, which immediately implies that $T_{ao}$ must increase when $T$ decreases. Also, with larger freshwater fluxes it is harder for the ocean to convect, so larger wind speeds are needed in order to avoid a collapse.

As mentioned earlier, the variables $q^*$, $R_H$, and $B_e$ are nonlinearly dependent on $T_{\text{air}}$ over the North Atlantic box. To solve the above equations we had to calculate these variables using $T_{ai}$, because $T_{ao}$, and therefore $T_{\text{air}}$, were unknown ahead of time. Using the above-calculated $T_{ao}$ to find the correct $T_{\text{air}}$, we corrected $q^*$, $R_H$, and $B_e$, and recalculated all five variables. There is no significant change in $S$, $T$, or $T_{ao}$. The volume flux $Q_1$ increased by 4 Sv and $F_H$ by 50 W m$^{-2}$, which constitutes approximately 20% of the originally calculated values. Finally, as mentioned, we implicitly assumed that, aside from the Ekman layers' heat exchange, the atmosphere can accept whatever heat the oceanic convection releases. This is plausible, as there are many ways in which it can be achieved (e.g., convection in the atmosphere or other means of entrainment), and it is in line with Eq. (2.7).

## 4. Inactive convection cell

With no convection in the North Atlantic, the convection condition (2.8) is dropped and we retain four equations [(2.1), (2.2), (2.3), and (2.10)], out of which (2.1) is inapplicable because no water is now sinking. To solve the remaining three equations [(2.2), (2.3), and (2.10)], we will assume that the oceanic temperature at the site corresponds to the low Heinrich events temperature shown in the Centre Européen de Recherche et d'Enseignement des Géosciences de l'Environnement (CEREGE) alkenone record (lower panel of Fig. 1). Accordingly, we take the oceanic temperature for the—now inactive—site to be 9°C, and we estimate the incoming eastward Sverdrup flow to the region to be roughly 20 Sv. Solving for $T_1$ and $T_{ao}$ in terms of $T$ and $Q_1$ for this nonconvective state gives us $T_1 = 10.4$°C and $T_{\text{ao}} = 0.4$°C. (Recalculating $q^*$, $R_H$, and $B_e$ for the

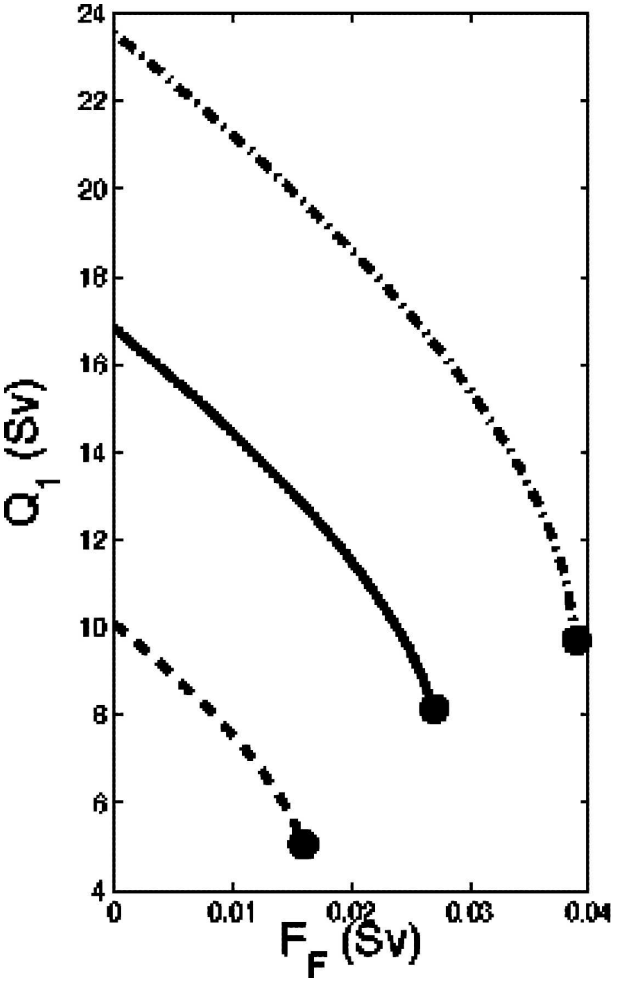


FIG. 7. As in Fig. 5, but for the convection-induced oceanic volume flux from the south $Q_1$. Since $F_F$ is small compared to $Q_1$, a similar plot for $W$ (not shown) is virtually indistinguishable from this plot.

correct $T_{\text{air}}$ gives us temperatures that vary little compared with those above.) Hence, with no convection, the ocean still cools by 1.4°C and still warms the atmosphere (by 5.4°C) but much less than it does with active convection (18°C). More importantly, however, in the collapsed case, no warm equatorial water ever reaches the high latitudes. The predicted collapse-induced changes in the oceanic and atmospheric temperature are shown with the difference in the horizontal lines in Fig. 1.

## 5. Discussion and summary

To simplify the introduction of our complete coupled model (Fig. 4), we first introduced a conceptual ultrasimple (one dimensional) chamber model (Fig. 2) that helps illustrate the counterintuitive heat-flux properties. This chamber model shows how the atmospheric and oceanic anomalies communicate and help explain the relationship between the oceanic and atmospheric horizontal temperature gradients. The general scenario of the complete coupled model is that, as the water approaches the convection site within the box (Fig. 4), Ekman layers provide the communication between the ocean and the atmosphere and help prepare the water for convection (by cooling it down to the required convective temperature). Once convection occurs, large amounts of other waters (superimposed on the Ekman flows) are drawn into the convection region.

The properties of the solution are discussed in detail in section 3. Here, they will only be briefly summarized. As expected, we find that there is a critical freshwater flux and a critical wind speed ($U_{10}$) above and below which the heat flux required for convection to occur cannot be dealt with. [This is consistent with the limit of $U_{10}$ going to zero, which, by virtue of (2.3), implies no convection.] At that point, the convection collapses and both the oceanic and atmospheric temperatures plunge (because equatorial water is no longer forced northward), in agreement with the numerical models mentioned in section 1. Mathematically, the collapsed states correspond to the condition that the square root associated with the solution of (3.3) becomes complex. These collapsed states are shown with the solid dots in Figs. 5–8, where the solution for subcritical freshwater values is also shown. We see that, as expected, the salinity at the site $S$, the ocean temperature at the convection site $T$, the transport of the MOC, the total heat flux to the atmosphere $F_H$, as well as the airflow mass transport $Q_{a1}$, all decrease with increasing freshwater flux $F_F$ at subcritical values. Also, with increasing freshwater flux, it is harder for the ocean to convect so a faster wind speed is needed to avoid a collapse.

We find that, for values below that catastrophic value, the outgoing air temperature $T_{ao}$ *increases* with increasing freshwater flux (Fig. 6). This counterintuitive increase is simply because the latent and sensible heat flux are primarily proportional to the temperature *difference* between the warm ocean and the cooler air, which must, therefore, decrease when the heat flux decreases. Since the ocean is warmer than the atmosphere, a decrease in the temperature difference between the two implies that the ocean cools and the atmosphere warms. This warming of the air is consistent with the Ekman coupling, which implies that, when the ocean cools down, the atmosphere must correspondingly warm up (according to the water/air heat capacity ratio).

For subcritical freshwater fluxes, both our model and

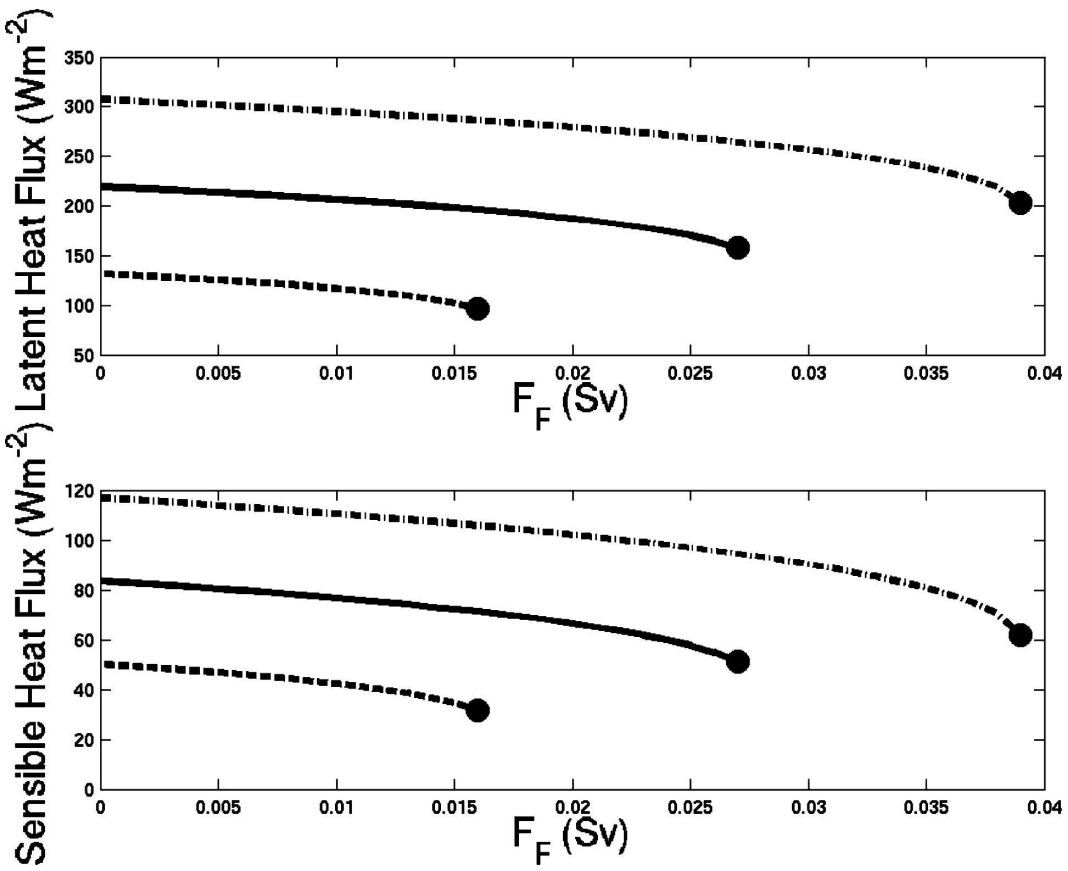


FIG. 8. As in Fig. 5, but showing the typical decomposition of the calculated heat flux into sensible and latent heat fluxes. As in present-day estimates for the North Atlantic, the latent heat flux is more than double the sensible heat flux.

the more complicated numerical models show a reduction in the MOC transport and a reduction in the heat flux to the atmosphere. However, with increased subcritical freshwater flux, the numerics show atmospheric cooling downstream whereas, as mentioned, our model shows warming (of a reduced amount of air). This is not a contradiction—the analytically predicted local warming of the reduced atmospheric mass flux is merely camouflaged by strong diffusion in the numerical atmosphere. Namely, the high diffusivities of the numerical atmosphere diffuse the *negative* heat-flux anomaly over a much greater area than it originally had, making it appear as a cooling of the surrounding air. With a horizontal diffusivity as high as $10^6$ $m^2 s^{-1}$, a flow above 500 km $\times$ 500 km convection area will be quickly (i.e., a few days) mixed into a much larger region with a resulting lower mean temperature.

To see this more clearly consider two adjacent eastward-flowing atmospheric jets of identical mass flux $Q$. One is flowing above the convection zone and exits with a (hypothetical) temperature anomaly $4\Delta T$ (above some mean) whereas the other is situated farther to the north and has a smaller temperature anomaly of $\Delta T$. Mixing the two together downstream yields a mean temperature anomaly of $2.5\Delta T$. Suppose now that the rate of freshwater flux increases so that the transport of the southern jet decreases to $0.25Q$ but its temperature anomaly increases to $5\Delta T$. The northern jet outside the convection region remains the same as before as it is not above the convection region. Mixing the two jets downstream now gives a mean temperature of $1.8\Delta T$, which is $0.7\Delta T$ *cooler* than before even though the southern jet *warmed* up by $\Delta T$.

The above-mentioned analytical property of atmospheric temperature increase due to increased freshwater flux points to an important instability process that might have been active during glaciation periods. Even the smallest freshwater flux causes local warming that, in turn, creates more melting and an ever-increasing freshwater flux. This process will continue until the collapsed state is reached (solid dots in Figs. 6–8). Of course, in order for this to happen, there must be plenty

of ice and snow around and this was true for the glaciation period but is not true today. This instability process is consistent with Tziperman's (1997) and others' result that the MOC was weaker and, hence, less stable during glaciation though it is not obvious what dynamics are active in these fairly complex numerical models.

Two additional points need to be made in regard to the critical freshwater flux (i.e., the freshwater flux needed to arrest convection). First, we found that, with our chosen values for the LGM, a freshwater event of $F_F > 0.03$ Sv would shut off convection, because the wind is not strong enough to transfer the required heat flux to the atmosphere. This calculated critical value is smaller than that seen to terminate convection in numerical models (e.g., Stouffer et al. 2006) primarily because our chosen LGM values have placed the system closer to a collapsed state, requiring a much smaller critical freshwater flux. Also, as mentioned earlier in the introduction, advection of water through the North Atlantic box, which spreads the anomaly around, is not included in our analytical model, and yet is included in numerical models. In addition, numerical models use relatively large vertical and horizontal diffusivities in the ocean (0.5–1.0 and $10^7$ cm$^2$ s$^{-1}$, respectively), introducing an additional 1–5-Sv flow through the region. Again, this requires numerical models to apply a larger freshwater flux for the same effect, as the freshwater anomalies are diffused away.

Second, Curry and Mauritzen (2005) calculated the amount of freshening that has occurred in the northern North Atlantic over the last 40 yr, from extensive hydrographic data in the region. They estimate a mean freshening of 0.02 ± 0.005 Sv over the entire period, with a drastic increase, during the late 1960s, of up to 0.06 Sv. Comparing the latter value to our critical freshwater flux, one can see that it is double the amount that our analytical model requires for a breakdown. This difference is because we use LGM values (rather than present-day values) in our calculation and this makes the system much more sensitive to freshwater fluxes. This is consistent with the idea that, during the LGM, the ocean was much closer to the critical fluxes than it is now (e.g., Labeyrie 2000). If modern-day values are used instead of the LGM values, the system breaks down for $F_F \geq 0.12$ Sv, well above the values Curry and Mauritzen (2005) found for the northern North Atlantic.

One can see from the paleoceanographic analysis shown in Fig. 1 and the superimposed analytical solution (horizontal lines) how our analytical results fall within the oceanic temperature range of what is considered Heinrich and non-Heinrich events, that is, nonconvective and convective states respectively. Thus, our analytical method and results can be seen as a first-order attempt to estimate the temperature change due to shifting convective states in the North Atlantic region.

*Acknowledgments.* The two reviewers (Eli Tziperman and Robbie Toggweiller) provided very useful comments even though they were not necessarily in agreement with our conclusions. We also thank Stephen Van Gorder for carefully reading a draft of this paper and providing insightful comments. Matthew Huber and Hezi Gildor also provided helpful comments. The National Aeronautics and Space Administration Grant NGT5-30513 and the National Science Foundation Grants OPP/ARC-0453846, OCE-0545204, and OCE-02421036 supported this study.

## APPENDIX

### List of Symbols and Abbreviations

| | |
|---|---|
| $A$ | Area of North Atlantic box (m$^2$) |
| $\alpha$ | Temperature expansion coefficient (K$^{-1}$) |
| $\beta$ | Salinity expansion coefficient (psu$^{-1}$) |
| $B_e$ | Bowen ratio |
| $C_{pa}$ | Heat capacity of air (J kg$^{-1}$ K$^{-1}$) |
| $C_{pw}$ | Heat capacity of seawater (J kg$^{-1}$ K$^{-1}$) |
| $C_S$ | Sensible-heat-flux constant |
| $C_L$ | Latent-heat-flux constant |
| $f_{1,2}$ | Coriolis parameters along the southern and northern island tips (s$^{-1}$, Fig. 2) |
| $F_f$ | Freshwater flux into the convection region (Sv) |
| $F_{Fc}$ | Critical freshwater flux (Sv) |
| $F_S$ | Sensible heat flux out of convection region (W m$^{-2}$) |
| $F_L$ | Latent heat flux out of convection region (W m$^{-2}$) |
| $F_H$ | Total heat flux out of the convection region (W m$^{-2}$) |
| $L_e$ | Latent heat of evaporation (J kg$^{-1}$) |
| $q^*$ | Saturation specific humidity (g kg$^{-1}$) |
| $\hat{Q}_a$ | Air volume flux in the chamber model |
| $\hat{Q}_w$ | Water volume flux in the chamber model oceanic transport into the box |
| $Q_{a1}$ | Atmospheric transport generated by the convection |
| $\tilde{Q}_w$ | Oceanic Ekman layer transport through the North Atlantic box (Sv) |
| $\tilde{Q}_a$ | Atmospheric Ekman layer transport through the atmospheric box (Sv) |
| $\rho_a$ | Mean density of air over the convection region (kg m$^{-3}$) |

| | |
|---|---|
| $\rho_w$ | Mean density of the water in the convection region (kg $m^{-3}$) |
| $\rho_0$ | Mean ocean water density (kg $m^{-3}$) |
| $R_H$ | Relative humidity |
| $S$ | Salinity of the water in the convection region (psu) |
| $S_1$ | Salinity associated with $Q_1$ (psu) |
| $S_D$ | Salinity of the deep layer (psu) |
| $T$ | Temperature of the water in the convection region (°C) |
| $T_1$ | Temperature associated with $Q_1$ (°C) |
| $T_D$ | Temperature of the deep layer (°C) |
| $T_{ai}$, $T_{ao}$ | Temperature of the incoming and outgoing air over the convection region (°C) |
| $T_{wi}$, $T_{wo}$ | Temperature of the incoming and outgoing water in the North Atlantic box (°C) |
| $U_{10}$ | Mean speed of atmosphere at 10 m |
| GISP | Greenland Ice Sheet Project |
| CEREGE | Centre Européen de Recherche et d'Enseignement des Géosciences de l'Environnement, Aix-en-Provence, France |

## REFERENCES


Adkins, J. F., K. McIntyre, and D. P. Schrag, 2002: The salinity, temperature, and $\delta^{18}O$ of the glacial deep ocean. *Science,* **298,** 1769–1773.

Bard, E., 2002: Climate shock: Abrupt changes over millennial time scales. *Phys. Today,* **55,** 32–38.

——, F. Rostek, J.-L. Turon, and S. Gendreau, 2000: Hydrological impact of Heinrich events in the subtropical northeast Atlantic. *Science,* **289,** 1321–1324.

Blunier, T., and Coauthors, 1998: Asynchrony of Antarctic and Greenland climate change during the last glacial period. *Nature,* **394,** 739–743.

Bond, G., W. Broecker, S. Johnsen, J. McManus, L. Labeyrie, J. Jouzel, and G. Bonani, 1993: Correlations between climate records from North Atlantic sediments and Greenland ice. *Nature,* **365,** 143–147.

Boyle, E. A., 2000: Is ocean thermohaline circulation linked to abrupt stadial/interstadial transitions? *Quat. Sci. Rev.,* **19,** 255–272.

Broecker, W. S., 1994: Massive iceberg discharges as triggers for global climate change. *Nature,* **372,** 421–424.

Cacho, I., J. O. Grimalt, C. Pelejero, M. Canals, F. J. Sierro, J. A. Flores, and N. Shackleton, 1999: Dansgaard-Oeschger and Heinrich events imprints in Alboran Sea paleotemperatures. *Paleoceanography,* **14,** 698–705.

Clark, P. U., N. G. Pisias, T. F. Stocker, and A. J. Weaver, 2002: The role of the thermohaline circulation in abrupt climate change. *Nature,* **415,** 863–869.

Curry, R., and C. Mauritzen, 2005: Dilution of the northern North Atlantic Ocean in recent decades. *Science,* **308,** 1772–1774.

De Boer, A. M., and D. Nof, 2004: The Bering Strait's grip on the Northern Hemisphere climate. *Deep-Sea Res. I,* **51,** 1347–1366.

Denton, G. H., R. B. Alley, G. C. Comer, and W. S. Broecker, 2005: The role of seasonality in abrupt climate change. *Quat. Sci. Rev.,* **24,** 1159–1182.

Fanning, A. F., and A. J. Weaver, 1997: Temporal-geographical meltwater influences on the North Atlantic conveyor: Implications for the Younger Dryas. *Paleoceanography,* **12,** 307–320.

Ganopolski, A., and S. Rahmstorf, 2001: Rapid changes of glacial climate simulated in a coupled climate model. *Nature,* **409,** 153–158.

——, and ——, 2002: Abrupt glacial climate changes due to stochastic resonance. *Phys. Rev. Lett.,* **88,** doi:10.1103/PhysRevLett.88.038501.

Gildor, H., and E. Tziperman, 2003: Sea-ice switches and abrupt climate change. *Philos. Trans. Roy. Soc. London,* **A361,** 1935–1944.

Gill, A. E., 1982: *Atmosphere–Ocean Dynamics*. Academic Press, 662 pp.

Hartmann, D. L., 1994: *Global Physical Climatology*. Academic Press, 411 pp.

Kaspi, Y., R. Sayag, and E. Tziperman, 2004: A "triple sea-ice state" mechanism for the abrupt warming and synchronous ice sheet collapse during Heinrich events. *Paleoceanography,* **19,** PA3004, doi:10.1029/2004PA001009.

Labeyrie, L., 2000: Glacial climate instability. *Science,* **290,** 1905–1907.

Li, C., D. S. Battisti, D. P. Schrag, and E. Tziperman, 2005: Abrupt climate shifts in Greenland due to displacements of the sea ice edge. *Geophys. Res. Lett.,* **32,** L19702, doi:10.1029/2005GL023492.

Loving, J. L., and G. K. Vallis, 2005: Mechanisms for climate variability during glacial and interglacial periods. *Paleoceanography,* **20,** PA4024, doi:10.1029/2004PA001113.

Manabe, S., and R. J. Stouffer, 1997: Coupled ocean-atmosphere model response to freshwater input: Comparison to Younger Dryas event. *Paleoceanography,* **12,** 321–336.

Marotzke, J., 2000: Abrupt climate change and thermohaline circulation: Mechanisms and predictability. *Proc. Natl. Acad. Sci. USA,* **97,** 1347–1350.

Nilsson, J., and G. Walin, 2001: Freshwater forcing as a booster of thermohaline circulation. *Tellus,* **53A,** 629–641.

Nof, D., I. McKeague, and N. Paldor, 2006: Is there a paleolimnological explanation for 'walking on water' in the Sea of Galilee? *J. Paleolimnol.,* **33,** 417–439.

Oberhuber, J. M., 1998: An atlas based on the COADS data set: The budgets of heat, buoyancy, and turbulent kinetic energy at the surface of the global ocean. Max-Planck-Institut für Meteorologie Rep. 15, 20 pp.

Paul, A., and M. Schultz, 2002: Holocene climate variability on centennial-to-millennial time scales: 2. Internal and forced oscillations as possible causes. *Climate Development and History of the North Atlantic Realm,* G. Wefer et al., Eds., Springer, 55–73.

Rahmstorf, S., 2002: Ocean circulation and climate during the past 120, 000 years. *Nature,* **419,** 207–214.

——, 2003: Thermohaline circulation: The current climate. *Nature,* **421,** 699.

——, and Coauthors, 2005: Thermohaline circulation hysteresis: A model intercomparison. *Geophys. Res. Lett.,* **32,** L23605, doi:10.1029/2005GL023655.

Sandström, J. W., 1908: Dynamische Versuche mit Meerwasser (Dynamical experiments with seawater). *Ann. Hydrogr. Marit. Meteor.,* **36,** 6–23.

——, 1916: Meteorologische studien im schwedischen Hochgebirge (Meteorological studies in the Swedish high moun-

tains). Goteborgs K. Vetensk. Vitterhets-Samh. Handl., Series 4, **22,** 1–48.

Saravanan, R., and J. C. McWilliams, 1995: Multiple equilibria, natural variability, and climate transitions in an idealized ocean–atmosphere model. *J. Climate,* **8,** 2296–2323.

Schiller, A., U. Mikolajewicz, and R. Voss, 1997: The stability of the North Atlantic thermohaline circulation in a coupled ocean–atmosphere general circulation model. *Climate Dyn.,* **13,** 325–347.

Schmidt, M. W., H. J. Spero, and D. W. Lea, 2004: Links between salinity variation in the Caribbean and North Atlantic thermohaline circulation. *Nature,* **428,** 160–163.

Seager, R., D. S. Battisti, J. Yin, N. Gordon, N. Naik, A. C. Clement, and M. A. Cane, 2002: Is the Gulf Stream responsible for Europe's mild winters? *Quart. J. Roy. Meteor. Soc.,* **128,** 2563–2586.

Stommel, H., 1961: Thermohaline convection with two stable regimes of flow. *Tellus,* **13,** 224–230.

Stouffer, R. J., and Coauthors, 2006: Investigating the causes of the response of the thermohaline circulation to past and future climate changes. *J. Climate,* **19,** 1365–1387.

Timmerman, A., H. Gildor, M. Schulz, and E. Tziperman, 2003: Coherent resonant millennial-scale climate oscillations triggered by massive meltwater pulses. *J. Climate,* **16,** 2569–2585.

Tziperman, E., 1997: Inherently unstable climate behaviour due to weak thermohaline ocean circulation. *Nature,* **386,** 592–595.

Wang, Z., and L. Mysak, 2006: Glacial abrupt climate changes and Dansgaard-Oeschger oscillations in a coupled climate model. *Paleoceanography,* **21,** PA2001, doi:10.1029/2005PA001238.

Yin, J. H., and D. S. Battisti, 2001: The importance of tropical sea surface temperature patterns in simulations of last glacial maximum climate. *J. Climate,* **14,** 565–581.